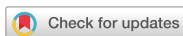


Original Article
Immunology



Evaluation of the immunobiological effects of a regenerative far-infrared heating system in pigs

Suji Kim ^{1,2}, Hong-Tae Park ^{1,2}, Sang Hee Soh ^{1,2}, Myung Whan Oh ^{1,2},
Sojin Shim ^{1,2}, Han Sang Yoo ^{1,2,3,*}

¹Department of Infectious Diseases, College of Veterinary Medicine, Seoul National University, Seoul 08826, Korea

²BK21 PLUS and Research Institute for Veterinary Science, College of Veterinary Medicine, Seoul National University, Seoul 08826, Korea

³BioMax/N-Bio Institute, Seoul National University, Seoul 08826, Korea



Received: Jul 15, 2019

Revised: Sep 6, 2019

Accepted: Sep 15, 2019

*Corresponding author:

Han Sang Yoo

Department of Infectious Diseases, BK21 PLUS and Research Institute for Veterinary Science, BioMax/N-Bio Institute, College of Veterinary Medicine, Seoul National University, 1 Gwanak-ro, Gwanak-gu, Seoul 08826, Korea. E-mail: yoohs@snu.ac.kr

© 2019 The Korean Society of Veterinary Science

This is an Open Access article distributed under the terms of the Creative Commons Attribution Non-Commercial License (<https://creativecommons.org/licenses/by-nc/4.0>) which permits unrestricted non-commercial use, distribution, and reproduction in any medium, provided the original work is properly cited.

ORCID iDs

Suji Kim 

<https://orcid.org/0000-0001-8901-0085>

Hong-Tae Park 

<https://orcid.org/0000-0003-3415-2339>

Sang Hee Soh 

<https://orcid.org/0000-0002-4675-3556>

Myung Whan Oh 

<https://orcid.org/0000-0002-7637-0644>

Sojin Shim 

<https://orcid.org/0000-0002-1769-0293>

Han Sang Yoo 

<https://orcid.org/0000-0003-0548-0835>

ABSTRACT

Thermal conditions are an important environmental factor in maintaining healthy pigs because they affect feed intake, growth efficiency, reproduction and immune responses in pigs. RAVI, a regenerative far-infrared heating system, can effect pig production by emitting an optimal far-infrared wavelength. Far-infrared radiation has been reported to increase microvascular dilation and vascular flow volume. The purpose of this study was to evaluate the immunobiological differences between pigs raised with the RAVI system and the gasoline heater system. Twenty-six-week-old weaned pigs were raised in two rooms that were equipped with a RAVI system or a gasoline heater for 8 weeks. A porcine atrophic rhinitis vaccine was administered after two weeks and transcriptome analysis in whole blood were analyzed at 2-week intervals. Signaling pathway analyses of the RAVI group at 8 weeks showed the activation of pathways related to nitric oxide (NO) production. This suggests that the application of RAVI might induce the production of NO and iNOS, which are important for increasing the immune activity. Similar to the result of microarray, phenotypic changes were also observed at a later period of the experiment. The increase in body weight in the RAVI group was significantly higher than the gasoline heater group at 8 weeks. The antibody titer against the vaccine in the RAVI group was also higher than that the gasoline heater group at 4 weeks and 8 weeks. This evaluation of the use of a far-infrared heating system with pigs will be helpful for applications in the pig farm industry and pig welfare.

Keywords: Far-infrared ray; pig; microarray; nitric oxide; immunobiological effect

INTRODUCTION

In a pig-raising environment, thermal conditions are one of the key factors that produce optimal conditions for pig production. Temperature fluctuations can cause stress in pigs that can lead to decreases in feeding, growth efficiency, reproduction, and immunity [1-4]. In particular, cold stress has been reported to increase mortality due to infectious disease in piglets [5,6]. The thermal environment is controlled by the interaction of air temperature,

Funding

This work was carried out with the support of “Cooperative Research Program of Center for Companion Animal Research (Project No. PJ013985012018)” Rural Development Administration, Republic of Korea.

Conflict of Interest

The authors declare no conflicts of interest.

Author Contributions

Conceptualization: Kim S, Park HT, Soh SH, Yoo HS. Formal analysis: Kim S, Park HT, Soh SH. Investigation: Kim S, Park HT, Soh SH, Oh MW, Shim S. Validation: Kim S, Park HT, Yoo HS. Writing - original draft: Kim S, Yoo HS. Writing - review & editing: Kim S, Yoo HS.

moisture, and airflow. A regenerative far-infrared heating system (RAVI) emits at an optimal far-infrared wavelength to aid in controlling pig-raising environment. RAVI uses a combination of nonmetallic heating element technology and nanocoated heat absorbing and radiating panel technology.

Far-infrared radiation (FIR) is nonionizing electromagnetic radiation with a wavelengths of 4–16 μm [7]. It is a source of high performance far-infrared rays that mainly exhibit thermal effects. FIR increases microvascular dilation and vascular flow volume and causes a slight elevation in the regional tissue temperature, reducing the sizes of water clusters by weakening the hydrogen bonds in water molecules [8-13]. Several studies have shown that far-infrared ray treatment promotes microcirculation and accelerates wound healing by increasing fibroblast proliferation, enhancing immunity by activating leukocytes and phagocytic processes, promoting sleep, and playing a prominent role in ameliorating aging processes [7,9,14-16]. For these reasons, FIR has been used as an alternative remedy in Japan, China, Taiwan, and Korea [15].

FIR modulates the innate immune defense system by stimulating nitric oxide (NO) production [15,17]. Recent studies have also reported that FIR enhances immunostimulatory activities, such as bactericidal and tumoricidal activities, by stimulating inducible nitric oxide synthetase (iNOS) [15,18]. iNOS enhances immune defense mechanisms, such as the phagocytic process, by producing large amount of NO [19]. NO is necessary for immunological responses to sources of infection, such as viruses, bacteria, fungi, protozoa, helminths, and tumor cells [9,20,21]. Although studies of iNOS expression in pigs have produced many contradictory results, several studies have detected iNOS production in many pig tissues [22-25].

Despite the many studies that have investigated the effects of FIR systems on mammals, the biological effects of FIR are not well understood. In this study, we investigated the biological effects of RAVI in pigs by evaluating body weight and, vaccination efficacy and performing transcriptomic analysis. Our results indicated that RAVI can increase body weight, enhance the efficacy of vaccines and regulate the immune response through NO production by iNOS in pigs. This study will be helpful in understanding the effects of a far-infrared radiant heating system in the context of the pig industry and welfare.

MATERIALS AND METHODS

Bioceramic material

RAVI is a far-infrared radiant heating system that combines nonmetallic heating element technology and the nanocoated heat absorbing and radiating panel technology (Ecopartners, Inc., Korea). It produces optimal far-infrared wavelength anions that barely affect moisture levels, ensuring fresh air even during lengthy use. It also minimizes the emission of fine dust, harmful substances, gases, and electromagnetic waves, ensuring fresh heated air through its antibacterial and deodorizing functions. The regenerative micro photogenic panel is a product that uses technology with high heat efficiency and the temperature of the surface area of a regenerative micro photogenic panel is approximately 350°C to 400°C, which is a higher surface temperature than that obtained in the same conditions in which luminous material is exposed.

Ethics statement

This experiment was carried out, in compliance with the Farm Animal Clinical Training and Research Center at Seoul National University. All procedures used for animal care and experiments were approved by the Seoul National University Institutional Animal Care and Use Committee (IACUC, Protocol #: SNU-160707-6).

Experimental design

Twenty of 6-week-old pigs were purchased from a commercial swine farm. The pigs were randomly divided without bias in terms of weight. Five pigs each were separated into one of four groups: the vaccinated RAVI group, the nonvaccinated RAVI group, the vaccinated gasoline group, and the nonvaccinated gasoline group. The pigs were raised in the presence of either a regenerative far-infrared heating system (RAVI) or a gasoline heater system (control). The animals were immunized twice at 2 weeks and 4 weeks with porcine atrophic rhinitis vaccine (TRICOM-Vac; Green Cross Veterinary Products Co., Korea) at a 1.5 mL dose via intramuscular injection. Whole blood was collected from the jugular vein in the pigs at 2-week intervals for 8 weeks. The body weight was measured 0, 2, 5 and 8 weeks.

RNA preparation, labeling and purification

Total RNA was isolated from the whole blood of experimental pigs using a PAXgene Blood RNA Kit (Qiagen, Germany) according to the manufacturer's protocol. Total RNA were processed with DNase digestion and clean-up procedures were performed. RNA purity and integrity were measured by the OD 260/280 ratio of ND-1000 spectrophotometer (NanoDrop, USA) for quality control. RNA were analyzed using the Agilent One-Color Microarray-Based Gene Expression Analysis protocol (Agilent Technology, V6.5 2010; Agilent Technologies, Inc., USA). 100 ng of total RNA was amplified and labeled with Cy3-dCTP. The cRNAs (pmol Cy3/ μ g cRNA) were purified by an RNeasy Mini Kit (Qiagen) and evaluated by a NanoDrop ND-1000 for identifying the concentration and specific activity.

Hybridization and scan

A total of 1,650 ng of each labeled cRNA was fragmented by adding 11 μ L 10 \times blocking agent and 2.2 μ L of 25 \times fragmentation buffer. The cRNA was heated at 60°C for 30 min and diluted with 55 μ L 2 \times GE hybridization buffer. One hundred microliters of hybridization solution was dispensed onto the gasket slide with a Agilent SurePrint HD Porcine GE 4X44K Microarray (Agilent). The slides were incubated for 17 h at 65°C in an Agilent hybridization oven. Then, the cells were washed at room temperature according to the Agilent One-Color Microarray-Based Gene Expression Analysis protocol (Agilent Technology, V6.5, 2010; Agilent Technologies, Inc.). The hybridized array was immediately scanned with an Agilent Microarray Scanner D (Agilent Technologies, Inc.).

Raw data preparation and statistical analysis

The microarray results were extracted using Agilent Feature Extraction software v11.0 (Agilent Technologies, Inc.). Array probes that had Flag A in the samples were filtered out. Selected gProcessedSignal values were transformed logarithmically and normalized by the quantile method. The significant data was determined by the LPE test and fold-change analysis for which the null hypothesis stated that no differences existed among the groups. The false discovery rate (FDR) was analyzed using the *p* value of the Benjamini-Hochberg algorithm. Hierarchical cluster analysis was performed by complete linkage and Euclidean distance as the measured of similarity for each DEG set. DEGs were analyzed using Gene enrichment and functional annotation based on the Gene Ontology database (www.geneontology.org/). All

data analysis and visualization of the differentially expressed genes were performed using R 3.1.2 (www.r-project.org).

Biological system analysis

Ingenuity Pathway Analysis (IPA; Ingenuity System Inc., USA) was performed for identifying the canonical pathways or functional processes in the DEGs. Significant DEGs were selected based on p value < 0.05 and fold change ≤ 1.5 for uploading the IPA program. The canonical pathway analysis was performed using a right-tailed Fisher's exact test. The significant pathway was determined by the ratio of the genes were mapped to the pathway and the p value measured by Fisher's exact test for calculating the probability of the association between the DEGs and the pathway.

Measurement of antibody titers

The values of the serum anti-*Bordetella bronchiseptica* antibody titers were determined by a microplate agglutination test (MAT) using the standard procedure with minor modifications. The serum samples were inactivated in 0.3% formalin and then two-fold serially diluted in PBS from 1:2 to 1:2,048. A total of 50 μ L of each serum dilution was added to the wells of a U-shaped microplate followed by the addition of antigens. The plate was incubated at RT overnight. Positive and negative sera were included as controls. The titers were expressed as the reciprocal of the highest dilution that showed agglutination.

Expression analysis of selected genes by real-time PCR

Five genes were selected to validate the microarray results based on showing differential expression by quantitative real-time PCR (qRT-PCR) (**Supplementary Table 1**). qRT-PCR reactions were performed with 1 μ L of cDNA using a Rotor-Gene SYBR Green PCR kit (Qiagen) and Rotor-Gene Q real-time PCR cycler (Qiagen). Amplification was performed for 35 cycles for 15 sec, at 95°C followed by 45 sec at 60°C, and the fluorescence was detected during the extension phase. The expression level was determined by the $2^{-\Delta\Delta Ct}$ method using glyceraldehyde-3-phosphate dehydrogenase (GAPDH) as a reference gene. The relative expression level was compared to that in control pigs to determine the fold change in expression for each gene.

Statistical analysis

The statistical significance of the differences was analyzed by Student's t -test or repeated measures ANOVA using GraphPad Prism version 7.00 for Windows (GraphPad Software, USA, www.graphpad.com). Genes were considered differentially regulated when $p < 0.05$. When the differences were determined to be significant, the fold-change with respect to the control condition was represented as follows: fold-change = mean ratio of gene expression in the RAVI group/mean ratio of gene expression in the gasoline group.

Data availability

The raw data files and normalized datasets are available from the Gene Expression Omnibus (GEO) at <https://www.ncbi.nlm.nih.gov/geo> under the accession number GSE131821.

RESULTS

Differentially expressed genes in pigs raised in the presence of RAVI and the gasoline heating system

cDNA microarrays were used to determine the transcriptome profiles for the analysis of signaling pathways involved in the immune regulation and metabolic process in the pigs raised with the RAVI system compared to those raised with the gasoline heating system. A total of 43,603 probes were present on the cDNA microarray. After normalization, 16,966 transcripts were identified in the RAVI and gasoline groups. According to a cut-off of 1.5 for fold-change and a p value < 0.05 , we identified 7,547 transcripts as significantly expressed. Hierarchical clustering showed that the 8W group was separated from 2W and 4W groups. The 8W RAVI group was found to have significantly differentially expressed genes when compared with the 8W gasoline heating group, whereas the 2W and 4W groups did not show significant differences in expression when compared with the gasoline heating group (**Fig. 1A**). Among the 7,547 transcripts identified, 238, 55 and 410 transcripts were significantly differentially expressed in the 2W, 4W and 8W RAVI groups. In scatter plot analyses of the DEGs, the 8W RAVI group showed the highest expression levels (**Fig. 1B**). The functional annotation of the 8W DEGs were analyzed in a gene set enrichment analysis of GO terms. Biological PANTHER annotation revealed that cellular and metabolic processes showed the highest enrichment in DEGs in the 8W group (**Supplementary Fig. 1**). The raw files and normalized datasets are available at the Gene Expression Omnibus (GEO) (<https://www.ncbi.nlm.nih.gov/geo/query/acc.cgi?acc=GSE131821>) under the accession number GSE131821.

Signaling pathway analysis of the 8W DEGs showed an association with NO production

Of the 16,966 DEGs, 8,176 genes were mapped to the Ingenuity Knowledge Base and were included according to the dataset filter (p value < 0.05). These DEGs were used in a core analysis carried out by using Ingenuity® Pathways Analysis (IPA, Ingenuity Systems, www.ingenuity.com). Canonical pathways were identified that were associated with the differentially expressed genes of the 8W RAVI group. Sixty-seven different canonical pathways in the 8W group were identified with significant differences [$-\log(p \text{ value}) \geq 1.3$] (**Table 1**). Among the significant signaling pathways in the 8W RAVI group, pathways related to NO production were predicted to be activated. “iNOS Signaling,” “MIF Regulation of Innate Immunity” and “Production of Nitric Oxide and Reactive Oxygen Species in Macrophages” were (z -score=1.342, 2 and 1,342). In these three pathways, iNOS was significantly activated and NO was predicted to be activated. CD14, FOS, LY96. and NOS2 were significantly activated in “MIF Regulation of Innate Immunity,” and CLU, FOS, NCF2, NOS2. and S100A8 were significantly activated in “Production of Nitric Oxide and Reactive Oxygen Species in Macrophages.” In the “iNOS Signaling” pathway, CD14, FOS, LY96, NOS2, and TRAF6 were significantly activated and TLR4, NF- κ B, STAT1, IRF1, and NO were predicted to be activated by the molecule activity predictor (MAP) (**Fig. 2**).

Evaluation of antibody production and body weight

All vaccinated groups showed a significant increase in the antibody titers against *B. bronchiseptica* 4 weeks post-immunization. The RAVI groups showed higher agglutination titers than the gasoline groups, although they were not increased significantly (**Fig. 3**). The body weight of pigs in the RAVI group was not significantly increased compared with gasoline group, however, the weight gain of pigs in the RAVI group showed a significant increase at 8 weeks (p value < 0.05) (**Fig. 4**).

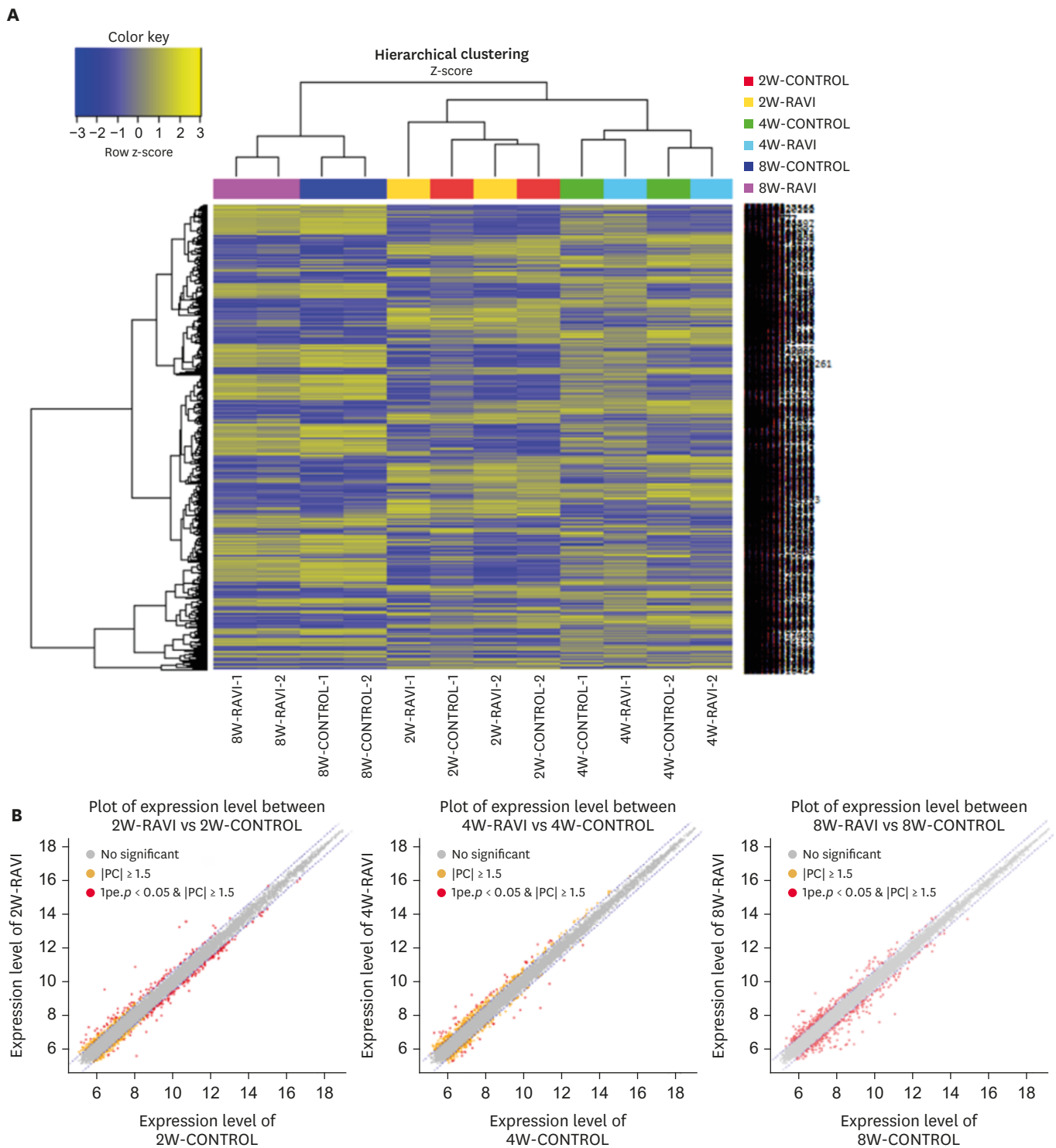


Fig. 1. Gene expression levels in the RAVI group compared with those in the gasoline group. (A) Hierarchical clustering analysis and (B) Scatter plot analysis. The blue dotted line indicates an expression level of $|fold\ change| \geq 1.5$. The red dotted line indicates an expression level with a p value < 0.05 . The expression levels were calculated using the base-2 logarithm of the normalized hybridization signals from each sample.

Table 1. Ingenuity pathway analyses of the RAVI group at 8 weeks

Ingenuity canonical pathways	-log(p value)	Ratio	z-score
Hepatic fibrosis/hepatic stellate cell activation	6.33	0.0526	-
IL-10 signaling	6.33	0.0959	-
Osteoarthritis pathway	5.79	0.0459	-1.414
LXR/RXR activation	5.73	0.0625	-1.890
IL-12 signaling and production in macrophages	5.17	0.0526	-
iNOS signaling	4.84	0.1040	1.342
Neuroinflammation signaling pathway	4.25	0.0305	1.265
Coagulation system	4.12	0.1140	1.000
Toll-like receptor signaling	3.84	0.0649	1.000
Acute phase response signaling	3.79	0.0393	0.447
Granulocyte adhesion and diapedesis	3.73	0.0385	-
Atherosclerosis signaling	3.71	0.0465	-
MIF regulation of innate immunity	3.69	0.0889	2.000
Agranulocyte adhesion and diapedesis	3.58	0.0363	-
ILK signaling	3.49	0.0352	-0.447
IL-8 signaling	3.38	0.0337	-0.378
Role of osteoblasts, osteoclasts and chondrocytes in rheumatoid arthritis	3.00	0.0290	-
Airway pathology in chronic obstructive pulmonary disease	2.95	0.2500	-
IL-17A signaling in fibroblasts	2.83	0.0857	-
IL-6 signaling	2.72	0.0368	1.000
Glucocorticoid receptor signaling	2.67	0.0227	-
Human embryonic stem cell pluripotency	2.53	0.0333	-
Role of IL-17A in psoriasis	2.51	0.1540	-
TGF- β signaling	2.50	0.0430	-1.000
cAMP-mediated signaling	2.40	0.0260	1.633
Hepatic cholestasis	2.25	0.0286	-
Role of macrophages, fibroblasts and endothelial cells in rheumatoid arthritis	2.25	0.0213	-
Sertoli cell-sertoli cell junction signaling	2.09	0.0262	-
Polyamine regulation in colon cancer	2.02	0.0870	-
Differential regulation of cytokine production in intestinal epithelial cells by IL-17A and IL-17F	2.02	0.0870	-
Production of nitric oxide and reactive oxygen species in macrophages	1.99	0.0248	1.342
Th1 pathway	1.91	0.0290	-
Cellular effects of sildenafil (Viagra)	1.84	0.0278	-
Glioma invasiveness signaling	1.84	0.0380	-
LPS/IL-1 mediated inhibition of RXR function	1.79	0.0219	1.000
Epithelial adherens junction signaling	1.77	0.0265	-
Iron homeostasis signaling pathway	1.77	0.0263	-
Ovarian cancer signaling	1.76	0.0261	-
MIF-mediated glucocorticoid regulation	1.65	0.0556	-
Tight junction signaling	1.63	0.0238	-
Cell cycle regulation by BTG family proteins	1.62	0.0541	-
NF- κ B activation by viruses	1.61	0.0312	-
Communication between innate and adaptive immune cells	1.60	0.0309	-
Relaxin signaling	1.58	0.0231	-
April mediated signaling	1.58	0.0513	-
Superpathway of citrulline metabolism	1.58	0.0513	-
CCR5 signaling in macrophages	1.58	0.0303	-
Colorectal cancer metastasis signaling	1.57	0.0192	0.447
Oncostatin M signaling	1.56	0.0500	-
Inhibition of matrix metalloproteases	1.56	0.0500	-
PPAR signaling	1.56	0.0297	-
B Cell activating factor signaling	1.54	0.0488	-
CXCR4 signaling	1.53	0.0222	-
Role of hypercytokinemia/hyperchemokininemia in the pathogenesis of influenza	1.50	0.0465	-
Th1 and Th2 activation pathway	1.47	0.0213	-
Gas signaling	1.45	0.0270	-
Type I diabetes mellitus signaling	1.44	0.0268	-
Thyroid cancer signaling	1.43	0.0426	-

(continued to the next page)

Table 1. (Continued) Ingenuity pathway analyses of the RAVI group at 8 weeks

Ingenuity canonical pathways	-log(p value)	Ratio	z-score
Dendritic cell maturation	1.41	0.0203	-
Graft-versus-host disease signaling	1.40	0.0408	-
Hematopoiesis from pluripotent stem cells	1.40	0.0408	-
G-protein coupled receptor signaling	1.39	0.0172	-
Autoimmune thyroid disease signaling	1.37	0.0392	-
Axonal guidance signaling	1.34	0.0139	-
Pancreatic adenocarcinoma signaling	1.33	0.0242	-
Role of cytokines in mediating communication between immune cells	1.32	0.0370	-
Neuroprotective role of THOP1 in Alzheimer's disease	1.32	0.0238	-

IL, interleukin; LXR, liver X receptor; RXR, retinoid X receptor; iNOS, inducible nitric oxide synthetase; MIF, macrophage migration inhibitory factor; ILK, integrin-linked kinase; TGF- β , transforming growth factor beta; cAMP, cyclic adenosine monophosphate; LPS, lipopolysaccharides; BTG family proteins; NF- κ B, nuclear factor kappa light chain enhancer of activated B cells; CCR5, C-C chemokine receptor type 5; PPAR, peroxisome proliferator-activated receptor; CXCR4, C-X-C chemokine receptor type 4; THOP1, thimet oligopeptidase 1.

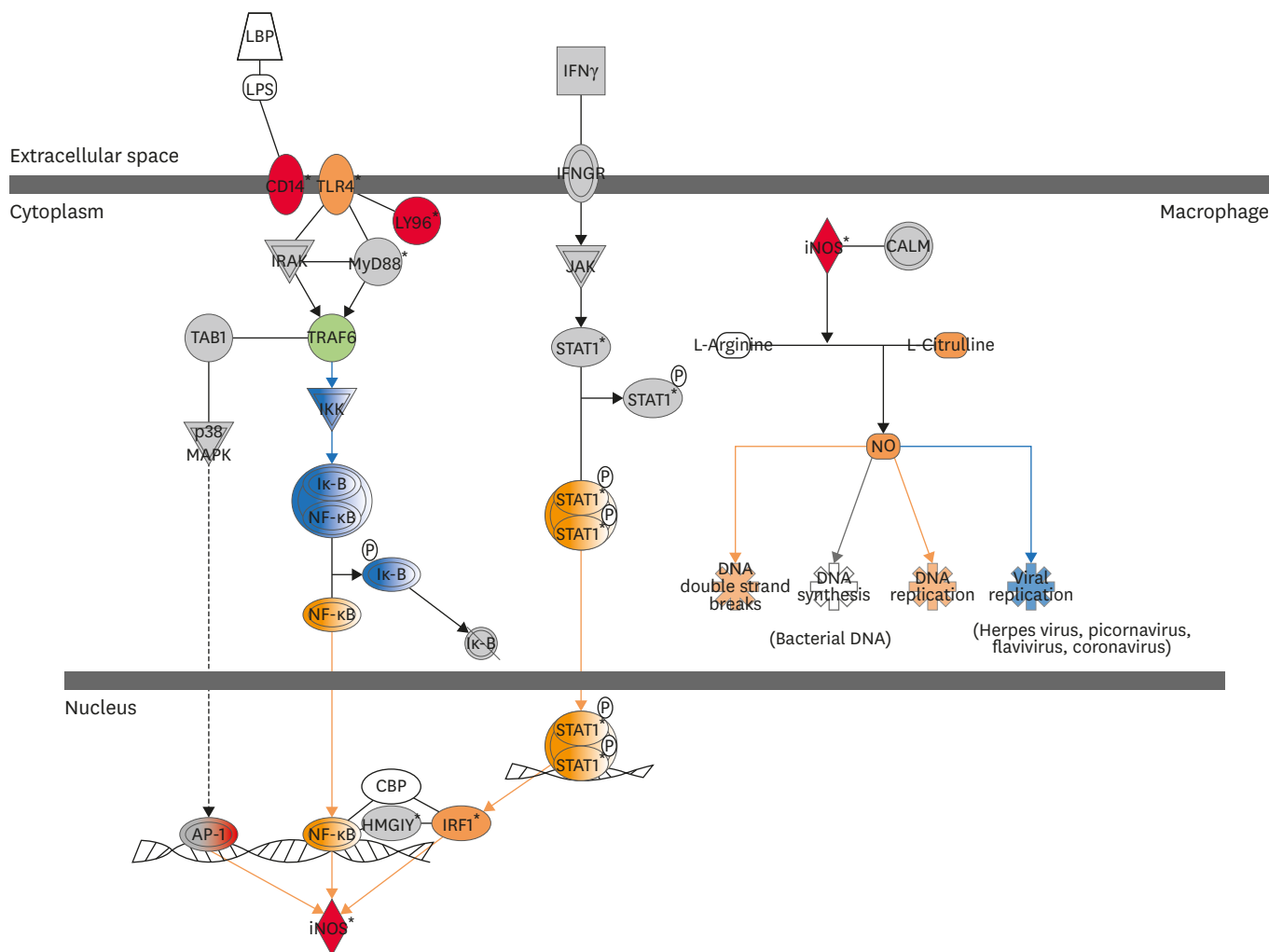


Fig. 2. Ingenuity pathway analyses of iNOS signaling in the 8W group. Red indicates upregulation, green indicates downregulation, orange indicates predicted activation, blue indicates predicted inhibition, and an uncolored node indicates that the genes were not differentially expressed in this pathway. The Ingenuity pathway analyses were generated through the use of IPA (QIAGEN Inc., <https://www.qiagenbioinformatics.com/products/ingenuity-pathway-analysis>). LPS, lipopolysaccharide; TLR4, toll-like receptor 4; iNOS, nitric oxide synthase; NF- κ B, nuclear factor kappa B; CBP, CREB-binding protein; IRF-1, interferon regulatory factor 1; AP-1, activator protein 1; STAT1, Signal transducer and activator of transcription 1; I κ -B, inhibitor of kappa B; TRAF6, tumor necrosis factor receptor-associated factor 6; CD14, cluster of differentiation 14; LY96, lymphocyte antigen 96; IRAK, interleukin-1 receptor-associated kinase; MYD88, myeloid differentiation primary response 88; TAB1, transforming growth factor-beta-activated kinase 1-binding protein 1; p38MAPK, mitogen activated protein kinase p38; IFN γ , interferon gamma; JAK, Janus kinase; CALM, clathrin assembly lymphoid myeloid leukemia; NO, nitric oxide.

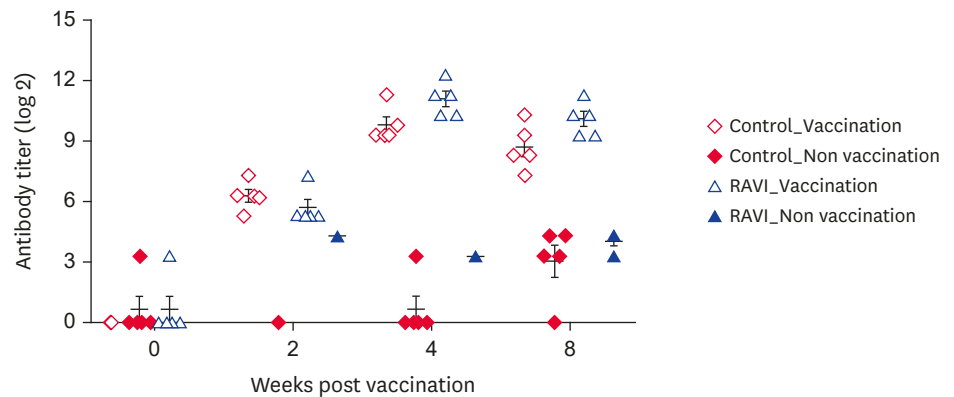


Fig. 3. Antibody titers against the *Bordetella bronchiseptica* in the RAVI group and the gasoline group. Antibody titers were determined by MAT. MAT was carried out using sera from nonvaccinated group and vaccinated group, of gasoline system (Control) and RAVI system. The data are shown as the geometric mean of titers in each group with the corresponding SD on a log₂ scale. MAT, microplate agglutination test; SD, standard deviation.

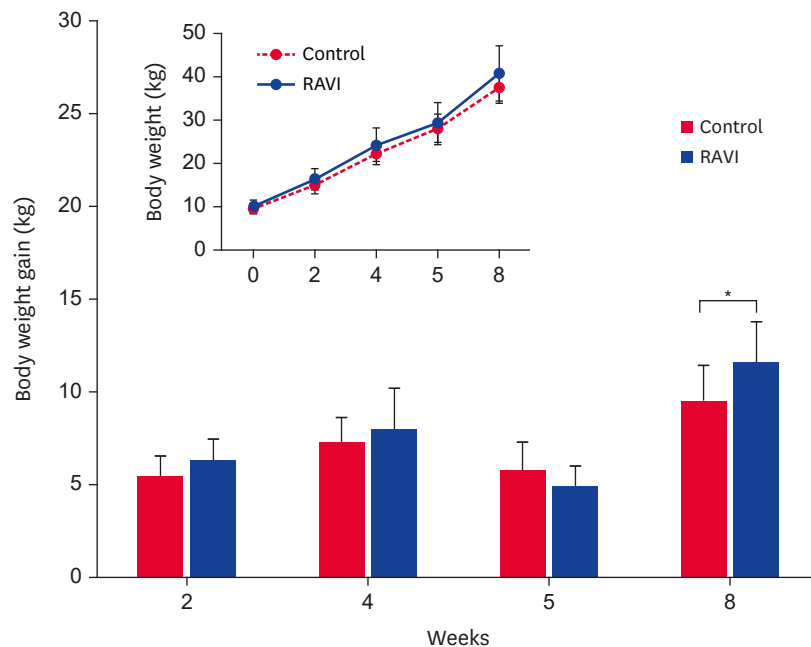


Fig. 4. The changes in the body weight of pigs raised in the presence of the RAVI system and the gasoline system. This graph indicates the body weight gain raised in the RAVI or gasoline systems between two body weight measurement times. The insert graph represent the body weight of pigs raised in the RAVI or gasoline systems. Data are expressed as means \pm standard error. Statistical difference indicates results compared the weight gain of the RAVI group with the gasoline group. * $p < 0.05$.

Validation of microarray results by qRT-PCR

RNA samples were assayed by quantitative real-time RT-PCR (qRT-PCR) to validate the microarray results. In the microarray results, the RAVI group showed significant changes in gene expression compared to the gasoline heater group. The upregulated genes CD14, CD163, CCR5, PTH1R, S1PR5, and SEMA6D and the downregulated gene GPX3 were selected to be assayed by qRT-PCR using the same RNA samples as those used for the microarray analysis. The correlation coefficient between the two analyses was 0.949. The differential

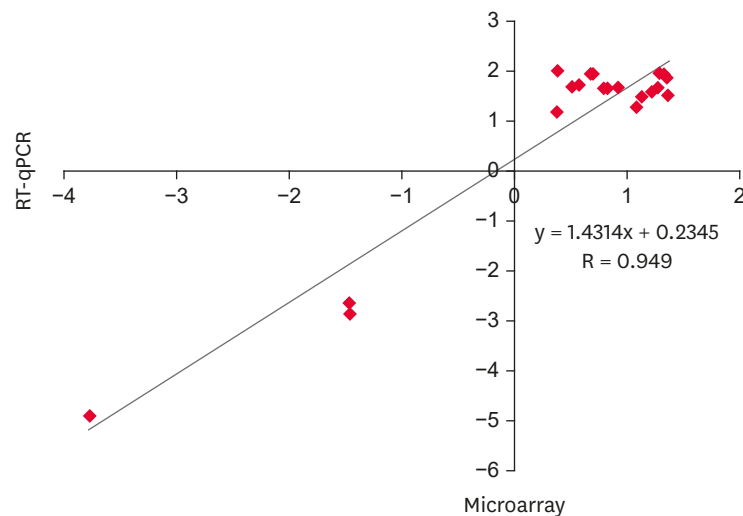


Fig. 5. Validation of gene expression by microarray assays and quantitative real-time PCR. The figure shows correlation between microarray and quantitative real-time PCR of mRNA expression. Quantification of mRNA is represented as a mRNA fold-change. The mRNA expression in the gasoline heater group at 0 week was considered as 1, as a reference for fold-change in expression. RT-qPCR, quantitative reverse transcription polymerase chain reaction; RT, reverse transcription; PCR, polymerase chain reaction.

expression of all selected genes was validated as the qRT-PCR results showed the same trends with respect to upregulation or downregulation (**Fig. 5**).

DISCUSSION

In the pig farming industry, control of the environment during weaning, commingling, crowding, and conditions of heat and cold is an important factor in pig production [1]. In particular, temperature fluctuations induce stress that causes weight loss and changes in growth efficiency and immune responses in pigs [2-4]. Cold stress has been reported as a main cause of morbidity and mortality in piglets [5,6]. In this study, RAVI, a far-infrared radiant heating system, was used to control the pig farm environment. After vaccination, pigs were raised for 8 weeks in the presence of the RAVI system or a gasoline heater system, which is what is usually used. In this period, body weight and immunostimulatory effects were evaluated and transcriptome analysis was performed to compare the effects of the RAVI system with those of the gasoline system.

In the transcriptome analysis, the DEGs in the 8W RAVI group were significantly differentially expressed only in comparison with those in the 2W and 4W RAVI groups. A gene set enrichment analysis of GO terms in the 8W RAVI group indicated that DEGs were highly enriched in cellular and metabolic processes according to the biological PANTHER annotation. The canonical pathway analysis also showed that the signaling pathways identified in the 8W RAVI group were related to the innate immune response. In particular, among these pathways, signaling pathways related to NO production in an iNOS-dependent manner such as “iNOS Signaling,” “MIR Regulation of Innate Immunity,” and “Production of Nitric Oxide and Reactive Oxygen Species in Macrophages,” were predicted to be activated. These three pathways commonly indicated that iNOS was likely activated and NO was predicted to be activated.

In the iNOS signaling pathway of the 8W RAVI group, CD14, LY96, AP-1, and iNOS were significantly activated and TLR4, NF- κ B, STAT1, IRF1 and NO were predicted to be activated. NO modulates the innate immune system by inhibiting pathogen replication [26]. A variety of extracellular stimuli can lead to expression of iNOS. For example, LPS from bacteria binds to LPS-binding protein. The binding of LPS activates transcription factors such as NF- κ B and AP-1, which mediate the expression of iNOS in immune and inflammatory responses [27-29]. TLR4 interacts with the CD14-LPS complex, and then TLR4 and CD14 modulate iNOS activity in the pro-inflammatory response via the activation of the NF- κ B pathway [30]. Interferon gamma (IFN- γ) also induces iNOS via the Jak-STAT signaling pathway. Activation of the Jak-STAT signaling pathway induces iNOS and NO production [31]. IFN- γ binds to IFN- γ R and phosphorylates STAT1, and then activated STAT1 increases iNOS induction and NO production. These pathways are important mechanisms underlying inflammatory processes and inflammatory disease [28].

Several studies have reported that FIR increases NO production by stimulating iNOS to enhance immunostimulatory activities [15-18]. Our study also showed an increase in NO production by iNOS stimulation in the 8W RAVI group after vaccination. However, the regulation of NO synthesis by iNOS can in different strains and species of animals and depends on the inducers that are activated. Bovine and murine macrophages generate considerable amounts of iNOS in response to cytokine stimulation, but human and pig macrophages are resistant [32]. Although studies of iNOS expression in pigs have shown contradictory results, many studies have detected iNOS and NO production in diverse pig tissues. Therefore, further studies are needed to clarify the production of NO and iNOS in pigs exposed to far-infrared rays.

FIR has been reported to increase microvascular dilation and tissue temperature by weakening the hydrogen bonds of water molecules by emitting at a wavelengths of 4–16 μ m as well as increasing NO production [7-13]. FIR also accelerates wound healing by increasing fibroblast proliferation, enhancing immunity by activating leukocytes and phagocytic processes, promoting sleep, and ameliorating the aging process [7,9,15,16]. Our results indicated that the body weight gain was significantly increased in pigs raised with a far-infrared radiant heating system. The microplate agglutination test also showed higher agglutination titers in the RAVI group compared with the gasoline group. Thus, these results indicated that a far-infrared radiant heating system might play a prominent role in increasing body weight and enhancing immunostimulating effects.

Although the effects of FIR have been investigated in many studies, the biological effects of a far-infrared radiant system have not been clearly identified. In this study, we evaluated the biological and immunostimulatory effects in pigs raised with a far-infrared radiant system. Our results indicated that body weight and vaccine efficacy were increased in the RAVI group, which raised the possibility of increasing NO production by exposing pigs to a far-infrared radiant heating system. This study will be helpful to enhance the welfare of pigs and the pig farming industry.

SUPPLEMENTARY MATERIALS

Supplementary Table 1

Primer sequences used for the real-time polymerase chain reaction measurements

[Click here to view](#)

Supplementary Fig. 1

GO analyses of annotated genes in the RAVI group. (A) 2w, (B) 4w, (C) 8w. The annotated genes were analyzed for the main biological processes GO-terms.

[Click here to view](#)

REFERENCES

1. Salak-Johnson JL, Webb SR. Pig social status and chronic cold or crowd stressors differentially impacted immune response. *Open J Anim Sci* 2018;8:280-293.
[CROSSREF](#)
2. Pennarossa G, Maffei S, Rahman MM, Berruti G, Brevini TA, Gandolfi F. Characterization of the constitutive pig ovary heat shock chaperone machinery and its response to acute thermal stress or to seasonal variations. *Biol Reprod* 2012;87:119.
[PUBMED](#) | [CROSSREF](#)
3. Ross J, Hale B, Gabler N, Rhoads R, Keating A, Baumgard L. Physiological consequences of heat stress in pigs. *Anim Prod Sci* 2015;55:1381-1390.
[CROSSREF](#)
4. Baumgard LH, Rhoads RP Jr. Effects of heat stress on postabsorptive metabolism and energetics. *Annu Rev Anim Biosci* 2013;1:311-337.
[PUBMED](#) | [CROSSREF](#)
5. Carroll JA, Burdick NC, Chase CC Jr, Coleman SW, Spiers DE. Influence of environmental temperature on the physiological, endocrine, and immune responses in livestock exposed to a provocative immune challenge. *Domest Anim Endocrinol* 2012;43:146-153.
[PUBMED](#) | [CROSSREF](#)
6. Carroll JA, Matteri RL, Dyer CJ, Beausang LA, Zannelli ME. Impact of environmental temperature on response of neonatal pigs to an endotoxin challenge. *Am J Vet Res* 2001;62:561-566.
[PUBMED](#) | [CROSSREF](#)
7. Lin YS, Lin MY, Leung TK, Liao CH, Huang TT, Huang HS, Pan HC. Properties and biological effects of high performance ceramic powder emitting far-infrared irradiation. *Instrum Today* 2007;6:60-66.
8. Yoo BH, Park CM, Oh TJ, Han SH, Kang HH, Chang IS. Investigation of jewelry powders radiating far-infrared rays and the biological effects on human skin. *J Cosmet Sci* 2002;53:175-184.
[PUBMED](#)
9. Leung TK, Lee CM, Lin MY, Ho YS, Chen CS, Wu CH, Lin YS. Far infrared ray irradiation induces intracellular generation of nitric oxide in breast cancer cells. *J Med Biol Eng* 2009;29:15-18.
10. Yu SY, Chiu JH, Yang SD, Hsu YC, Lui WY, Wu CW. Biological effect of far-infrared therapy on increasing skin microcirculation in rats. *Photodermatol Photoimmunol Photomed* 2006;22:78-86.
[PUBMED](#) | [CROSSREF](#)
11. Inoué S, Kabaya M. Biological activities caused by far-infrared radiation. *Int J Biometeorol* 1989;33:145-150.
[PUBMED](#) | [CROSSREF](#)
12. Leung TK, Lin SL, Yang TS, Yang JC, Lin YS. The influence of ceramic far-infrared ray (cFIR) irradiation on water hydrogen bonding and its related chemo-physical properties. *Hydrology* 2014;5:2.
13. Leung TK, Huang PJ, Chen YC, Lee CM. Physical-chemical test platform for room temperature, far-infrared ray emitting ceramic materials (cFIR). *J Chin Chem Soc* 2011;58:653-658.
[CROSSREF](#)
14. Ishibashi J, Yamashita K, Ishikawa T, Hosokawa H, Sumida K, Nagayama M, Kitamura S. The effects inhibiting the proliferation of cancer cells by far-infrared radiation (FIR) are controlled by the basal expression level of heat shock protein (HSP) 70A. *Med Oncol* 2008;25:229-237.
[PUBMED](#) | [CROSSREF](#)
15. Leung TK, Lin YS, Chen YC, Shang HF, Lee YH, Su CH, Liao HC, Chang TM. Immunomodulatory effects of far-infrared ray irradiation via increasing calmodulin and nitric oxide production in raw 264.7 macrophages. *Biomed Eng (Singapore)* 2009;21:317-323.
16. Leung TK. *In vitro* and *in vivo* studies of the biological effects of bioceramic (a material of emitting high performance far-infrared ray) irradiation. *Chin J Physiol* 2015;58:147-155.
[PUBMED](#)

17. Gavish L, Perez LS, Reissman P, Gertz SD. Irradiation with 780 nm diode laser attenuates inflammatory cytokines but upregulates nitric oxide in lipopolysaccharide-stimulated macrophages: implications for the prevention of aneurysm progression. *Lasers Surg Med* 2008;40:371-378.
[PUBMED](#) | [CROSSREF](#)
18. Smallwood HS, Shi L, Squier TC. Increases in calmodulin abundance and stabilization of activated inducible nitric oxide synthase mediate bacterial killing in RAW 264.7 macrophages. *Biochemistry* 2006;45:9717-9726.
[PUBMED](#) | [CROSSREF](#)
19. Bogdan C. Nitric oxide and the immune response. *Nat Immunol* 2001;2:907-916.
[PUBMED](#) | [CROSSREF](#)
20. Daff S. Calmodulin-dependent Regulation of Mammalian Nitric Oxide Synthase. Portland Press Limited, London, 2003.
21. Weber TJ, Smallwood HS, Kathmann LE, Markillie LM, Squier TC, Thrall BD. Functional link between TNF biosynthesis and CaM-dependent activation of inducible nitric oxide synthase in RAW 264.7 macrophages. *Am J Physiol Cell Physiol* 2006;290:C1512-C1520.
[PUBMED](#) | [CROSSREF](#)
22. Kim H, Moon C, Ahn M, Lee Y, Kim H, Kim S, Ha T, Jee Y, Shin T. Expression of nitric oxide synthase isoforms in the porcine ovary during follicular development. *J Vet Sci* 2005;6:97-101.
[PUBMED](#) | [CROSSREF](#)
23. Cohen RI, Hassell AM, Ye X, Marzouk K, Liu SF. Lipopolysaccharide down-regulates inducible nitric oxide synthase expression in swine heart *in vivo*. *Biochem Biophys Res Commun* 2003;307:451-458.
[PUBMED](#) | [CROSSREF](#)
24. Zelnickova P, Matiasovic J, Pavlova B, Kudlackova H, Kovaru F, Faldyna M. Quantitative nitric oxide production by rat, bovine and porcine macrophages. *Nitric Oxide* 2008;19:36-41.
[PUBMED](#) | [CROSSREF](#)
25. Mathewson AM, McPhaden AR, Wadsworth RM. The induction and detection in vitro of iNOS in the porcine basilar artery. *J Immunol Methods* 2003;279:163-171.
[PUBMED](#) | [CROSSREF](#)
26. Medzhitov R. Toll-like receptors and innate immunity. *Nat Rev Immunol* 2001;1:135-145.
[PUBMED](#) | [CROSSREF](#)
27. Xia YF, Liu LP, Zhong CP, Geng JG. NF-kappaB activation for constitutive expression of VCAM-1 and ICAM-1 on B lymphocytes and plasma cells. *Biochem Biophys Res Commun* 2001;289:851-856.
[PUBMED](#) | [CROSSREF](#)
28. Aktan F. iNOS-mediated nitric oxide production and its regulation. *Life Sci* 2004;75:639-653.
[PUBMED](#) | [CROSSREF](#)
29. Lowenstein CJ, Padalko E. iNOS (NOS2) at a glance. *J Cell Sci* 2004;117:2865-2867.
[PUBMED](#) | [CROSSREF](#)
30. Schröder NW, Opitz B, Lamping N, Michelsen KS, Zähringer U, Göbel UB, Schumann RR. Involvement of lipopolysaccharide binding protein, CD14, and Toll-like receptors in the initiation of innate immune responses by *Treponema* glycolipids. *J Immunol* 2000;165:2683-2693.
[PUBMED](#) | [CROSSREF](#)
31. Rao KM. Molecular mechanisms regulating iNOS expression in various cell types. *J Toxicol Environ Health B Crit Rev* 2000;3:27-58.
[PUBMED](#) | [CROSSREF](#)
32. Jungi TW, Adler H, Adler B, Thöny M, Krampe M, Peterhans E. Inducible nitric oxide synthase of macrophages. Present knowledge and evidence for species-specific regulation. *Vet Immunol Immunopathol* 1996;54:323-330.
[PUBMED](#) | [CROSSREF](#)